

## USE OF THE CONTINUITY PRINCIPLE TO EVALUATE WATER PROCESSING RATE OF SUSPENSION-FEEDING MOSQUITO LARVAE

J. O. LACOURSIÈRE,<sup>1</sup> C. DAHL<sup>2</sup> AND L.-E. WIDAHL<sup>2</sup>

**ABSTRACT.** Water processing rates of active suspension-feeding larvae of *Culiseta morsitans* and *Culex quinquefasciatus* 2nd and 4th instars were estimated through video image analysis of the conical jet flow driving the large recirculation patterns surrounding the organisms. In accordance with the principle of continuity, individual processing rates (PRs) were assessed by averaging a series of consecutive flow rates ( $Q_c$ ) defined as the product of the water velocity ( $U_c$ ) and the associated cross-sectional area ( $A_c$ ) along a transect passing through the center of the delineated jet flow. Results clearly show very tight adherence to the principle of continuity. They also demonstrate that, although extreme care must be taken when streamtube delineation is performed, the methodology used can generate reliable assessment of individual processing rates regardless of the instars or species studied. The small coefficient of variation observed in assessing PR at the larval level further underlines the consistency of the method. Significant differences in water processing rates were observed for different species and instars. These could partially be related to body size, head width, and the length of the lateral palatal brushes (LPBs), which are the structures involved in the production of the water jet. Assessment of the jet velocity at the feeding groove level suggests the key role of LPB beating frequency in the jet intensity, and consequently the magnitude of the processing rate. Analysis of data further indicates that obligate suspension feeders such as *Cs. morsitans* must sustain a larger flow pattern around the larvae to ensure sufficient particle entrapment than facultative suspension feeders (or even brushers) such as *Cx. quinquefasciatus*.

**KEY WORDS** Principle of continuity, flow pattern, water processing rate, suspension feeders, Culicidae

### INTRODUCTION

Under lotic conditions, the particle flux through filtering structures of passive suspension feeders is known to depend on particle concentration, local flow velocities, filtering structure morphology, and passive or active filter orientation toward the incoming flow (Joergensen 1983; Cheer and Koehl 1987; Loudon 1990; Lacoursière and Craig 1993; Shimeta and Koehl 1995, 1997). However, under lentic conditions, particle encounter is, in addition to particle concentration, governed by a behaviorally sustained flow pattern, which is mainly dependent on the size and beating or pulsating frequency of the structure generating it, as well as by the complex 3-dimensional funneling flow path conveying the particles to the filtering structures (Dahl et al. 1988, Vanderploeg 1990, Shimeta and Jumars 1991, Merritt et al. 1992b, Widahl 1992, Vogel 1994). Assessment of filter-feeding efficiency, traditionally defined as the ratio of the number of ingested particles to the number that passes through the filtering structure, requires knowledge of the particle flux and filtering rate to determine the number of incident particles. In active suspension feeders such as mosquito larvae, such estimates are complicated by the constant change in free-hanging positions and the complex recirculation patterns surrounding the organisms.

In the past, filtration rates of mosquito larvae were indirectly estimated from particle removal

rates out of defined water volumes and time intervals (Dadd 1968, 1971; Aly 1988; Rashed and Mulla 1989). For example, when fed on latex beads, significant differences in filtration rate were observed between 4th-stage larvae of *Aedes aegypti* (L.) (0.164–0.192  $\mu\text{l}/\text{sec}$ ), *Culex quinquefasciatus* Say (0.136–0.164  $\mu\text{l}/\text{sec}$ ), *Anopheles albimanus* Wied. (0.014–0.015  $\mu\text{l}/\text{sec}$ ), and *Anopheles quadrimaculatus* Say (ca. 0.009  $\mu\text{l}/\text{sec}$ ) (Aly 1988). However, such assessment of filtration rates dictates that all test organisms filter at a constant pace through the entire time interval (Joergensen 1983, Aly 1988) and that particles do not settle differently, hence not accounting for inter- and intraspecific behavioral variations or for differences in particle sink rates related to variances in convective flow cell patterns.

Widahl (1992) demonstrated that the driving force behind the large flow cell patterns observed in larvae of *Culiseta morsitans* (Theobald) and *Aedes communis* (De Geer) was the strong central jet (referred to as alpha flow) having a well-defined origin at the feeding groove. The 3-dimensional flow pattern draws particle-laden water from all direction toward the feeding groove (Widahl 1992, Figs. 1–3) where the particles are accelerated away from the head by the effect of a jet. Particles stop almost immediately when the jet ceases, without exhibiting inertia, indicating that a low Reynolds number ( $Re$ ) governs flow circulation (Dahl et al. 1988, Merritt et al. 1992a). Although flow pattern generation is known to be under the influence of filament length and stroke frequency of lateral palatal brushes (LPBs), the relative involvement of other structures such as mouthpart setae and the pharynx is still under debate (Dahl et al. 1988, Merritt et al. 1996). However, Widahl (1994) has clear-

<sup>1</sup>Lund University, Limnology Department, Ecology Building, Sölvegatan 37, S-223 62 Lund, Sweden.

<sup>2</sup>Uppsala University, Evolutionary Biology Center, Department of Systematic Zoology, Norbyvägen 18 D, S-752 36 Uppsala, Sweden.

ly demonstrated that shortened LPB filaments significantly reduce the size of the generated flow pattern.

If we assume that all particles passing in the immediate vicinity of the feeding groove are conveyed by the strong central jet, as videotape and microcinematography analyses strongly suggest (Widahl 1992, Merritt et al. 1996), the diameter and velocity of that jet therefore can be used to calculate a processing rate. As the principle of continuity (White 1986) dictates, the flow rate ( $Q_x$ ), which is the product of cross-sectional area ( $A$ ) and average velocities ( $U$ ) normal to the plane of that area, is the same anywhere between rigid walls or flow streamlines (i.e.,  $Q = A_1U_1 = A_2U_2 = A_xU_x \dots$  where subscripts denote locations along the stream flow). In an open flow field, under laminar conditions, that is low  $Re$ , streamlines are analogous to the rigid walls of pipes (Vogel 1994). Hence, fluid is automatically prohibited from crossing streamlines forming the streamtube so that if streamlines diverge, fluid must slow down; conversely if streamlines converge, fluid must accelerate. Consequently, as the water within the jet decelerates as distance from the feeding groove increases, the diameter of the jet must expand accordingly. An average water processing rate (PR) can therefore be calculated from the various locations within the boundary of the jet (Fig. 1B). Lacoursière and Craig (1993) have successfully used this principle to determine the amount of water processed by larval fans of simuliid larvae.

The main goal of this paper is to demonstrate that the principle of continuity can be used to assess the water PR of individual mosquito larvae. The use of 4 different groups of larvae will allow us to explore if the PR is dependent on body size or LPB size, and thus is species and instar specific.

## MATERIALS AND METHODS

Experiments were conducted with 2nd and 4th larval instars of *C. quinquefasciatus* and *Cs. morsitans*. *Culex quinquefasciatus* (Cq) were from a laboratory colony maintained as in Dahl et al. (1993), whereas *Cs. morsitans* (Cm) were field collected and stored at 10°C in indigenous water containing small quantities of fish fry food (Tetra®) as a supplement diet. Before experiments, larvae of both species were starved in distilled filtered water (0.22 µm, Millipore, Sundryberg, Sweden) for 15–18 h at maintenance temperature, and then acclimated for 4–8 h at 14°C until 2 h before the experiment when they were transferred to room temperature (20°C). Four groups were therefore investigated in this experiment: 2nd instars of *Cx. quinquefasciatus* (Cq<sub>II</sub>), 4th instars of *Cx. quinquefasciatus* (Cq<sub>IV</sub>), 2nd instars of *Cs. morsitans* (Cm<sub>II</sub>), and 4th instars of *Cs. morsitans* (Cm<sub>IV</sub>).

Observations were made on a single larva placed into a small crystal vial (10 mm wide × 10 mm

deep × 15 mm high for the 2nd instars; 27 mm wide × 27 mm deep × 15 mm high for the 4th instars) containing distilled, Millipore-filtered water. A mixture of cellulose particles of ca. 20-µm diameter, yeast powder, and Na-fluorescein or carmine red (Saturnus®) dye was then added with a long-needle syringe near the bottom of the cell. Feeding activity and particle or tracer displacement (Fig. 1B) were recorded with a Panasonic® color video camera (model CCD F10) mounted on a dissecting scope (Wild® M5A, 6× magnification), and a Panasonic video cassette recorder (model AG-7330). Illumination was provided by fiber-optic light (Intralux® Fot 150, Ch 8957 Spreitenbach, Switzerland). Trace measurements were taken from a Panasonic color video monitor, using frame-by-frame analysis (1 frame = 0.02 sec) and were calibrated using a finely graduated ruler recorded at all magnifications. The focal plane was always maintained on the cephalic capsule, and only video segments showing lateral views of the larvae were selected for analysis.

As larvae initiated suspension-feeding, particles and tracer were entrained from the bottom of the cell and incorporated into the induced flow patterns described by Dahl et al. (1988) and Widahl (1992). Individual trace particles, selected for their focal stability and their position within or at the edge of the jet, were analyzed as their distance from the feeding groove increased (minimum of 3 traces/particle). The presence of the color dye was used to facilitate and confirm the delineation of the jet flow.

In accordance with the principle of continuity, an individual PR was assessed by averaging a series of consecutive  $Q_x$ s defined as the product of  $U_x$  and the associated  $A_x$  along a transect passing through the center of the jet flow (Fig. 1B, where subscript annotations refer to individual volumetric cross-sections along the conical jet flow). Only particles traveling on the focal plane near the center of the jet flow were selected for this analysis. After identification of a suitable video recording segment, jet dimensions, arbitrarily delineated by the zone of high velocity shear rendered visible by the sharp changes in particle trajectory lengths, were determined by fast forward–fast rewind playback analysis of particle and dye circulation. Streamline boundaries of the jet flow were sketched directly on the monitor screen and the selected trace particles were analyzed. Water velocity ( $U_x$ ) was calculated from the particle's displacement ( $d_x$ ), magnification factor for the monitor, and the video camera shutter speed (0.02 sec, i.e., 0.04 sec between frames). Cross-sectional area was calculated from the diameter ( $D_x$ ) of the conical jet flow, where  $D_x$  was always assessed at the center of the  $d_x$  path, at which the distance from the head (DFH<sub>x</sub>) was also measured (Fig. 1B).

Individual PR was calculated by averaging a series of  $Q_x$ s, each being estimated from ca. 3 trace particles observed at ca. 15 locations along the jet

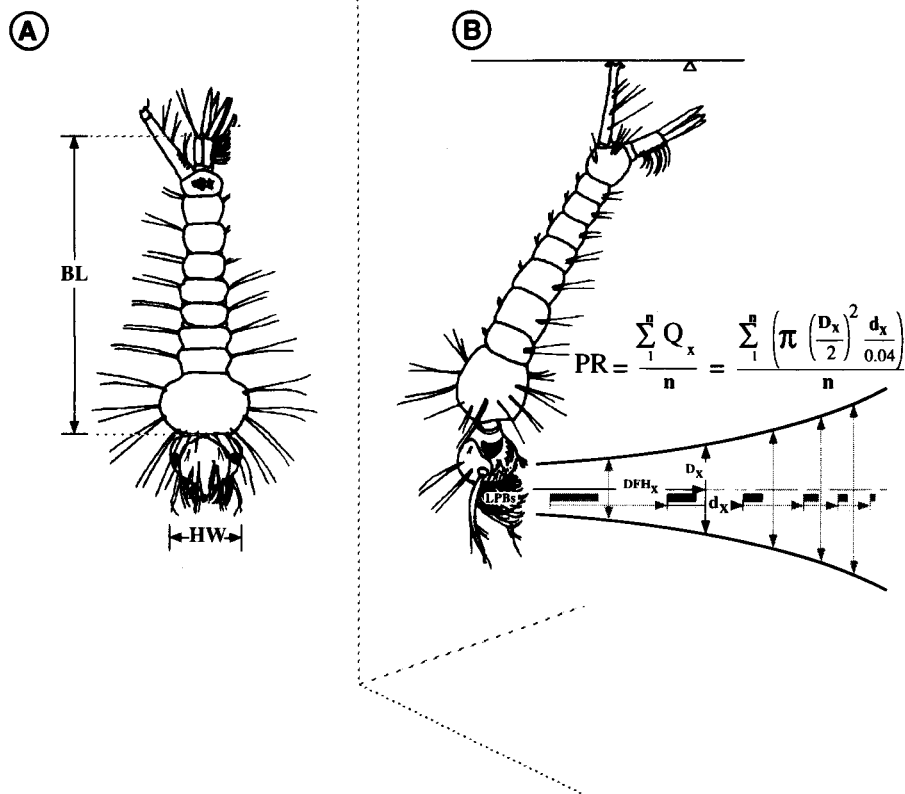


Fig. 1. Schematic representation of the parameters used in assessing and relating processing rate (PR). A. Larval body length (BL) and head width (HW). B. Conical jet flow sustained by the lateral palatal brushes (LPBs), where subscript annotations refer to individual volumetric cross-sections along the jet;  $d_x$  is the distance traveled by a particle as estimated from the displacement of the trace origin between 2 video frames (i.e., 0.04 sec), as the particle distance from the head ( $DFH_x$ ) increases;  $D_x$  is the diameter of the jet flow delineated by 2 flowlines (see text for procedure);  $n$  is the number of calculated flow rates ( $Q_x$ ) defined as the product of the streamtube area ( $\pi [0.5d_x]^2$ ) and the local flow velocity ( $d_x/0.04$ sec).

flow (i.e., ca. 45 points, 25 video frames, 0.5 sec) until the distance from the head had reached at least one body length. As larvae often feed in brief intermittent cycles, suitable trace particles may originate from different feeding activities, and streamtube dimensions must be redelineated accordingly. Average PRs for instar and species were estimated from a total 492 observations (22 particles for 10 larvae) for  $Cm_{II}$ , 233 observations (17 particles for 7 larvae) for  $Cm_{IV}$ , 381 observations (21 particles for 7 larvae) for  $Cq_{II}$ , and 476 observation (26 particles for 11 larvae) for  $Cq_{IV}$ . In compliance with the continuity principle, to maintain  $Q_x$  constant within a streamtube, the streamtube  $A$  must increase as its internal velocity ( $U$ ) decreases. Because the rate at which this change occurs is dependent on the prevailing  $Q$  (Fig. 2A), standardization of  $A$  and  $U$  (Fig. 2B) is necessary to allow comparisons of dimensions observed from different conditions (i.e., particles, larvae, instar, and species), hence com-

pensating the effect of size variation between instars and species. Evaluation of the concurrent changes in jet flow velocity and diameter for conformity to the principle of continuity is therefore performed with standardized variables, where each value in a parameter set (i.e., parameter values derived from different particles, larvae, instars, and species) was divided by the maximum value observed in that set (Figs. 2C, 2D).

Reliability and possible limitations of the estimation method were further tested by plotting the calculated PRs ( $Q_x$ s) against the  $DFH_x$  at which they were estimated, and by analyzing the resulting regression slope in each of the 4 cases studied for their conformity to the null hypothesis (i.e., slope = 0) (Fig. 3).

Morphologic measurements were made on microscope slide preparations of ethanol-fixed larvae. With exception of  $Cs_{II}$  that were from the same habitat but of a different batch, all larvae measured

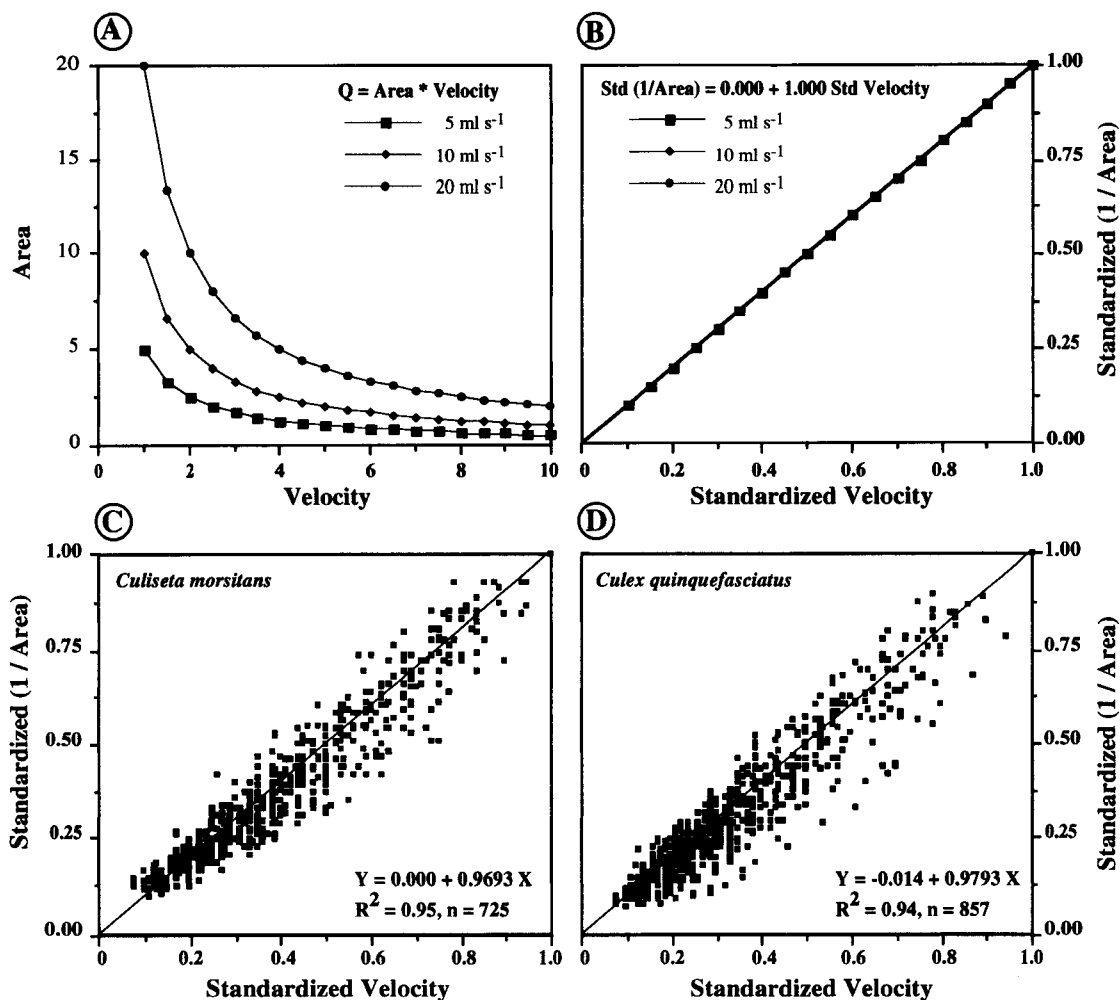


Fig. 2. Principle of continuity. A. Theoretical representation of the relationship between area and velocity along streamtubes of different discharge ( $Q$ ). B. Linear model of the principle of continuity, for standardized streamtubes of different discharge. C. Standardized dimensions along the jet flows of both 2nd and 4th instars of *Culiseta morsitans* (total of 17 larvae). D. Standardized dimensions along the jet flows of both 2nd and 4th instars of *Culex quinquefasciatus* (total of 18 larvae).

came from the respective samples used in the experiment. Body length (BL) is defined as the distance between the end of the anterior thorax and the posterior margin of segment X (Fig. 1A). Head capsule width (HW), head capsule length (HL), and LPB filament lengths are defined as in Widahl (1988).

Statistical analyses and multivariate and non-parametric analyses were performed using the statistical package SYSTAT version 5.2 for the Macintosh (SYSTAT, Inc.).

## RESULTS

As dictated by the principle of continuity, a linear relationship close to unity is observed between standardized area ( $1/A$ ) and velocity for both *Cs.*

*morsitans* and *Cx. quinquefasciatus*, respectively, demonstrating coefficients of 0.969 and 0.979 (Figs. 2C, 2D). Such close adherence to the expected relationship indicates that  $Q_x$ s assessed from single particle trajectory within the central portion of the jet flow should remain constant within the boundary of the streamtube of suspension-feeding mosquitoes, regardless of their larval instars. As shown in Fig. 3, a certain variation in estimated  $Q_x$  is observed within each group analyzed and, although present only in 2 of the 4 cases, a small positive trend in larger  $Q_x$  estimates is present as DFH increases. When analyzing PR estimates from single particle trajectories ( $\text{PR} = Q_x$  average), the coefficient of variation (CV) observed is ca. 10% (range: 4.5–20%), regardless of the particle, and remains at that level (range: 0.5–27%) when esti-

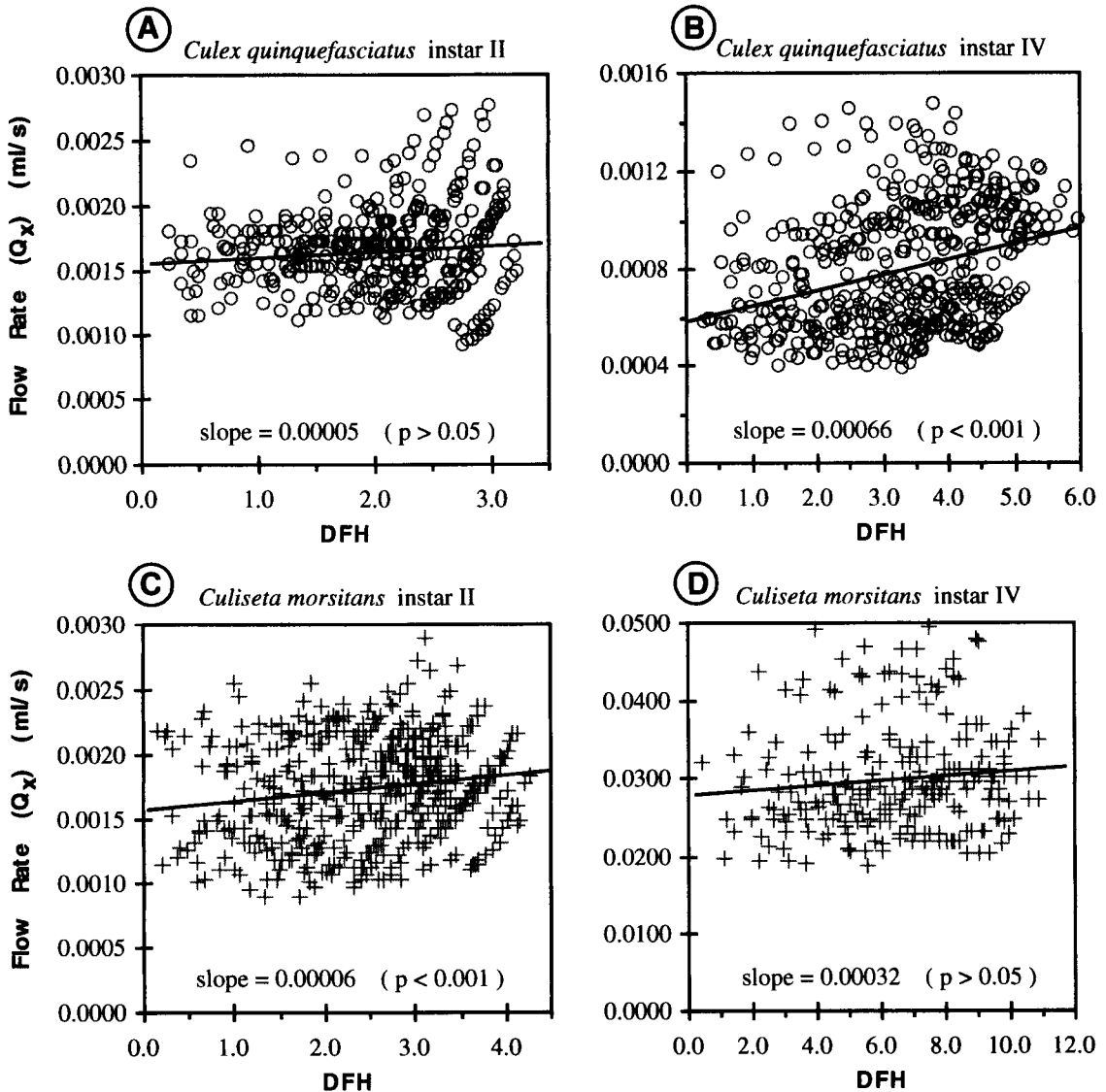


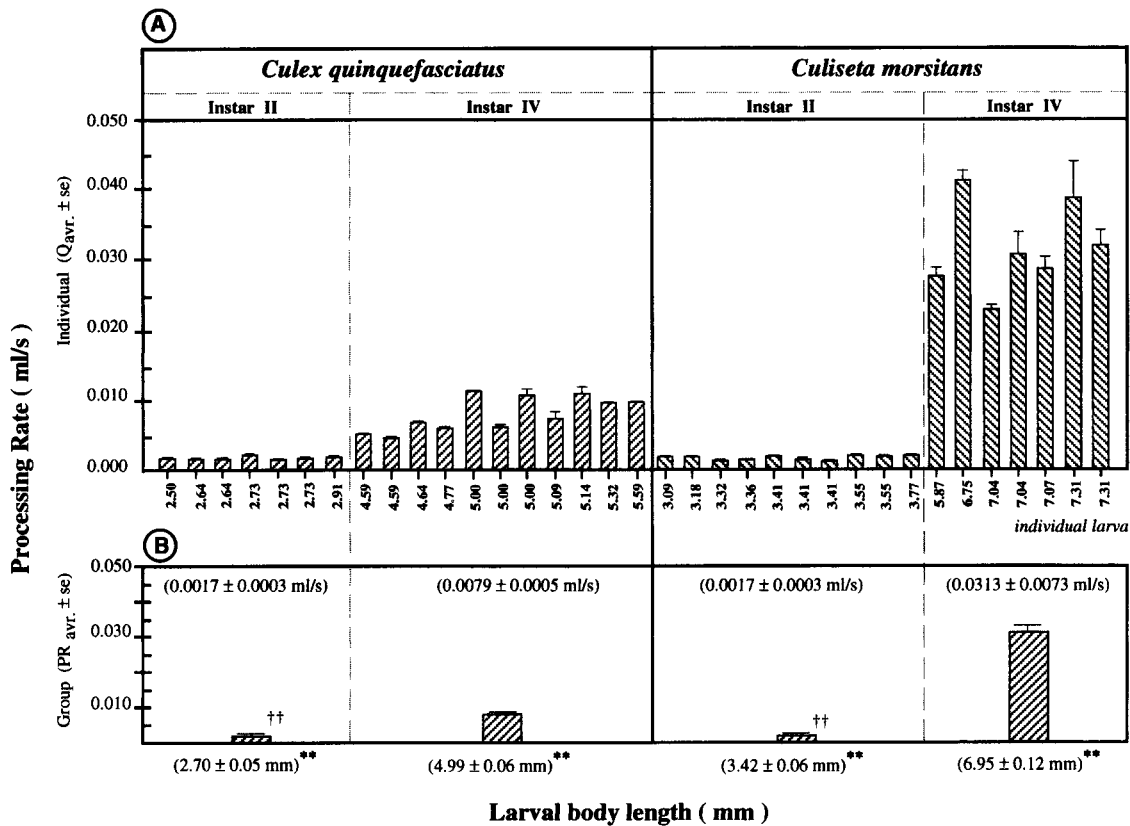
Fig. 3. Variation in calculated flow rates ( $Q_x$ ) as distance from the head (DFH) increases for (A) 2nd and (B) 4th instars of *Culex quinquefasciatus*, and for (C) 2nd and (D) 4th instars of *Culiseta morsitans*. Note the different scales between the different axes.

mates from trajectories are combined to assess individual larval PR, regardless of the larva considered. If estimates from trajectories are pooled to assess an average PR for an instar, the associated CV increases to ca. 24% (20.2–31.9%).

Variation in  $Q_x$  observed within groups is reflected in the individual PR assessment (Fig. 4), which ranged between 1.4 and 2.1  $\mu\text{l}/\text{sec}$  for  $Cq_{II}$  ( $1.7 \pm 0.3 \mu\text{l}/\text{sec}$ , mean  $\pm$  SD), 5.3 and 11.4  $\mu\text{l}/\text{sec}$  for  $Cq_{IV}$  ( $7.9 \pm 0.5 \mu\text{l}/\text{sec}$ ), 1.2 and 2.0  $\mu\text{l}/\text{sec}$  for  $Cm_{II}$  ( $1.7 \pm 0.3 \mu\text{l}/\text{sec}$ ), and 22.8 and 41.1  $\mu\text{l}/\text{sec}$  for  $Cm_{IV}$  ( $31.3 \pm 7.3 \mu\text{l}/\text{sec}$ ). Within each group, larvae of similar BL can demonstrate significantly different PRs (Fig. 4A). Even if trends of higher PR with

longer BL seem to exist in some groups, only  $Cq_{IV}$  has demonstrated a small ( $r^2 = 0.42$ ) but significant ( $P = 0.002$ ) relationship. In all other cases, although resolutions of measurement techniques are reliable, no relationships with BL are found (all  $r^2 < 0.007$ ; all  $P > 0.5$ ). Changes in PR between instars are species specific. For a similar increase in BL between the 2nd and the 4th instars of *Cx. quinquefasciatus* and of *Cs. morsitans* (ca. 1.9  $\times$  and 2.0  $\times$ , respectively), a 1.85-fold increase between  $Cq_{II}$  and  $Cq_{IV}$  is observed (ANOVA,  $P < 0.001$ ) compared to an 18.4-fold increase between  $Cm_{II}$  and  $Cm_{IV}$  ( $P < 0.001$ ) (Fig. 4B).

When analyzed as a larval assemblage, a strong



(average ± standard error)

\*\* significant differences (p < 0.001) in average species body length

†† no significant differences in average species processing rate, all other comparisons significantly different (p ≤ 0.001)

Fig. 4. Estimated processing rates of 2nd and 4th instars of *Culiseta morsitans* and *Culex quinquefasciatus* larvae in relation to their body length. A. Individual larvae processing rates (i.e., average flow rates Q<sub>x</sub>); B. Group average processing rates.

sigmoid relationship can be found between individual PR and BL (PR = 0.034 - 0.0002BL<sup>3</sup> + 0.0043BL<sup>2</sup> - 0.0222BL; limits: 2.5 and 7.5 mm; r<sup>2</sup> = 0.90; P = 0.06; Fig. 5A). However, BL alone is not necessarily a good predictor of overall PR, as demonstrated by 2nd instars of *Cs. morsitans* and *Cx. quinquefasciatus*, which, although significantly different in length (BL of Cq<sub>II</sub> = 0.79BL of Cm<sub>II</sub>; P < 0.001), have identical PR (ca. 1.7 μl/sec). Individual PR also demonstrates a significant sigmoid relationship with larval (HCW) (PR = 0.159 - 0.123HCW<sup>3</sup> + 0.443HCW<sup>2</sup> - 0.474HCW; limits: 0.7 and 1.8 mm; r<sup>2</sup> = 0.93; P = 0.06; Fig. 5B), where for similar HCW both Cq<sub>II</sub> and Cm<sub>II</sub> demonstrate identical PRs. A similar relationship is also observed with larval HCL. Overall relationship between individual PRs and filament lengths of the LPBs, the beating structures driving the flow pattern, cannot be upheld because instars of similar LPB filament lengths (i.e., Cm<sub>II</sub> and Cq<sub>IV</sub>) clearly demonstrate distinct processing rates (Fig. 5C).

When considering jet flow characteristics (Fig. 6), concurrent analyses of changes in jet velocities and diameters as DFH increases reveal that larvae of *Cs. morsitans* generate stronger and more focused jet flows than those of *Cx. quinquefasciatus*. Rapid deceleration and expansion of a jet flow is characterized by a steep negative relationship between jet central velocities and associated DFH (Fig. 6A) and a steep positive relationship between the jet diameters and associated DFH (Fig. 6B). Conversely, shallow relationships (i.e., regression slopes tend toward zero) are characteristic of stronger and more focused jet flows. Because of the limitation in shutter speed of the recording equipment, jet flow characteristics at the feeding groove level can only be obtained by extrapolating the observed relationships to the head plane (i.e., DFH = 0, the regression constant). From Table 1, it can be noted that the estimated diameter of the jet flow in the immediate vicinity of the feeding groove seems to be only partially influenced by head geometry,

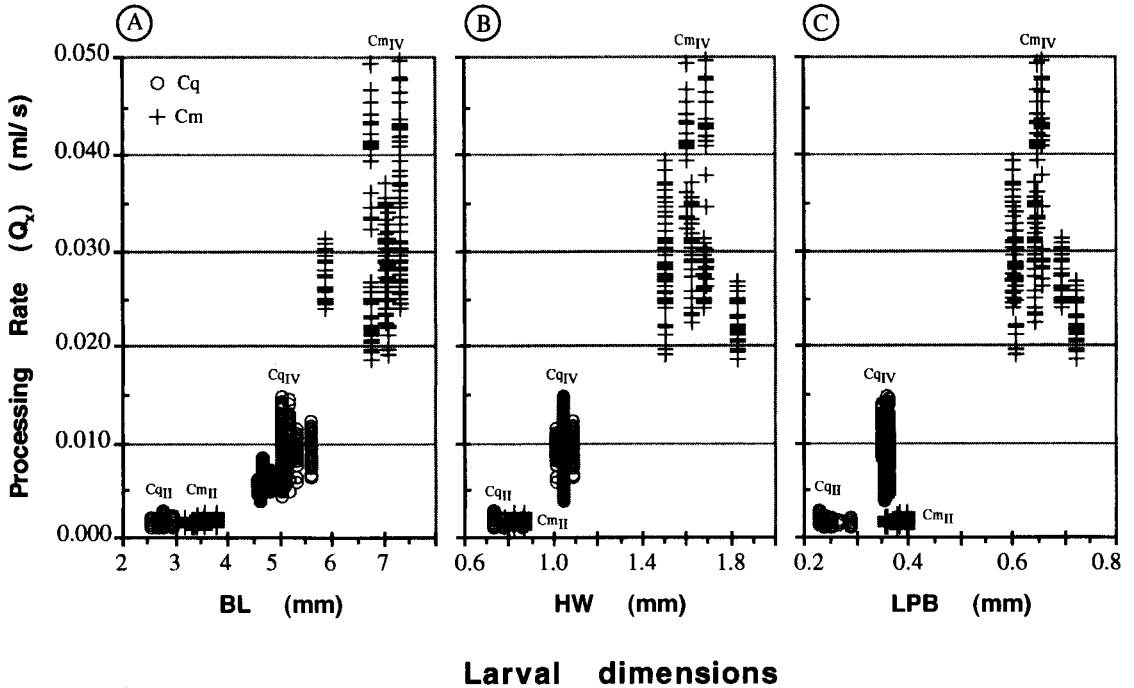


Fig. 5. Processing rates, as expressed by individual flow rates ( $Q_x$ ), in relation to larval (A) body length (BL); (B) head width (HW); and (C) lateral palatal brushes (LPBs) filament length.

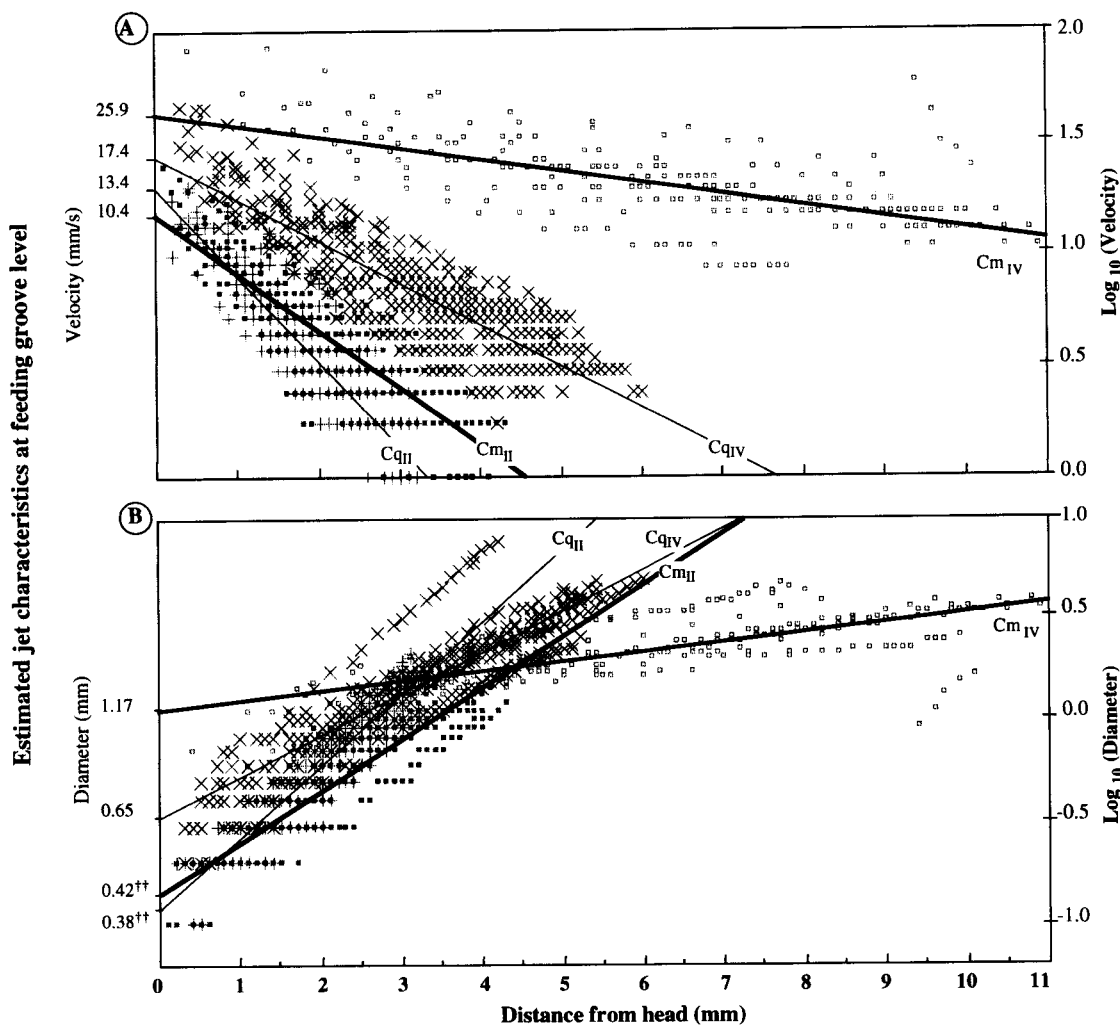
whereas the velocities cannot be explained by LPB filament lengths alone. Although no quantitative measurements were performed, jet flow velocity was observed to slightly change as the LPB's beating frequency varied, with a higher frequency generating stronger flows. It was also noted that jet flow diameter slightly varied as maxillae or mandibles positions changed, also slightly affecting the jet velocity.

## DISCUSSION

Results from this study demonstrate that measurements taken from jet flows of active suspension-feeding larvae are in close adherence to the theoretical relationship defined by the principle of continuity. The technique clearly establish that particles travelling on the focal plane near the center and at the edge of the jet flow provide reliable determination of both water velocity and streamtube boundary. These in turn generate relatively constant  $Q_x$  assessments as indicated by the low CV observed in estimating individual PRs. In most instances, estimates of  $Q_x$  have remained quite constant along the delineated streamtube, although a small positive trend was observed for 4th instars of *Cx. quinquefasciatus* and 2nd instars of *Cs. moritans* as DFH increased. Further analyses of individual particle traces revealed that, in some instances,  $Q_x$  shows an increase as distances exceed ca. 75–80% of the definable streamtube length, sug-

gesting limiting PR assessments to the 1st  $\frac{2}{3}$  of the streamtubes. Nevertheless, because estimates of  $Q_x$  are quite often made from particles of different feeding cycles (i.e., because of low numbers of suitable particles with optimal trajectories within a single video segment), the small CV observed in assessing individual PRs from different streamtubes further underlines the consistency of the method. However, although independent analyses repeated by different individuals on the same video segments have shown the reliability of the procedure, one must consider that precision (i.e., decrease in CV and consistency of  $Q_x$  with DFH) increases with the observer's experience.

The increase in CVs observed when estimating average PRs at the instar level most likely demonstrates small individual variations more than estimation procedure effects. Exploration of inter- and intraspecific variations in PRs strongly suggests that some morphological and behavioral parameters are critical in defining and controlling the central jet flow, which drives the recirculation pattern surrounding the larva, and hence the amount of processed particles. Within each of the 4 groups studied, the lack of a clear relationship between PR and BL might be partly influenced by the small variations in BL observed between newly molted and older larvae. The small variations in individual PRs observed within each group are most likely the result of intrinsic variability in sclerotized structures such as the head and the filament length of the



†† No significant differences ( $p > 0.05$ )

Fig. 6. Estimation of the jet flow dimensions at the feeding groove level for 2nd and 4th instars of *Culiseta morsitans* (Cm<sub>II</sub> and Cm<sub>IV</sub>, respectively) and 2nd and 4th instars of *Culex quinquefasciatus* (Cq<sub>II</sub> and Cq<sub>IV</sub>, respectively). A. Initial jet velocity extrapolated from the variation in observed jet velocity (log<sub>10</sub> scale) as the distance from the head decreases. B. Initial expulsion jet diameter extrapolated from the variation in observed jet diameter (log<sub>10</sub> scale) as the distance from the head decreases.

LPBs. Differences in PRs observed with variations in HCW, HCL, and filament length of LPBs strongly indicate the influence of head morphology on the jet flow diameter at the feeding groove level. The relationship between the LPB length and  $Q_x$  further attests to behavioral influence as (although no quantitative observations were made) the diameter and velocity of the jet were observed to slightly change as maxillae or mandible positions and the LPB's beating frequency varied. Consequently, in this experiment, analysis of data suggests that identical PRs observed between Cq<sub>II</sub> and Cm<sub>IV</sub>, which have similar HCW, could be due to a lower beating frequency of the longer LPBs of Cm<sub>II</sub>, as suggested

by the lower jet flow velocity observed at the feeding groove level of Cm<sub>II</sub> than Cq<sub>II</sub> larvae (Fig. 6B). Conversely, the higher PR observed for Cq<sub>IV</sub> when compared to Cm<sub>II</sub> larvae, which possess similar LPB length, could be explained by a wider flow jet (i.e., wider head capsule) as well as a higher LPB beating frequency, as indicated by the higher jet flow velocity observed at the feeding groove level. Analysis of the data further indicates that, as suggested by the slope of the relationship between jet flow velocities and DFH (i.e., the smaller the slope, the more powerful the flow jet as water velocity is maintained further from the head), obligate suspension feeders such as *Cs. morsitans* can sustain a

Table 1. Larval and jet flow characteristics of 2nd instars and 4th instars of *Culex quinquefasciatus* (Cq<sub>II</sub> and Cq<sub>IV</sub>, respectively) and 2nd and 4th instars of *Culiseta morsitans* (Cm<sub>II</sub> and Cm<sub>IV</sub>, respectively).<sup>1</sup>

	Cq <sub>II</sub>		Cm <sub>II</sub>		Cq <sub>IV</sub>		Cm <sub>IV</sub>
Larval characteristics							
Body length (mm)	2.69	<	3.44	<	5.01	<	6.86
Head capsule width (mm)	0.77	=	0.81	<	1.04	<	1.63
Head capsule length (mm)	0.54	<	0.59	<	0.81	<	1.18
LPB filament length (mm)	0.25	<	0.37	=	0.36	<	0.65
Processing rate (ml/sec)	0.017	=	0.0017	<	0.0080	<	0.0301
Jet flow characteristics							
Diameter at feeding groove (mm)	0.387	=	0.431	<	0.650	<	1.159
Velocity at feeding groove (mm/sec)	13.4	>	10.5	<	17.3	<	25.9
Regression slope (log[D <sub>x</sub> ] vs. DFH)	0.173	>	0.129	=	0.100	>	0.025
Regression slope (log[U <sub>x</sub> ] vs. DFH)	-0.339	≅	-0.227	=	-0.162	>	-0.045

<sup>1</sup> > or <,  $P < 0.05$ ;  $\geq$  or  $\leq$ ,  $P < 0.10$ ; =,  $P > 0.10$ ; LPB, lateral palatal brush; D<sub>x</sub>, diameter of the conical jet flow; DFH, distance from the head.

larger flow pattern around the larvae than facultative suspension feeders (or even browsers) such as *Cx. quinquefasciatus* (slope of  $-0.225$  and  $-0.045$  for Cm<sub>II</sub> and Cm<sub>IV</sub>, respectively, and of  $-0.339$  and  $-0.163$  for Cq<sub>II</sub> and Cq<sub>IV</sub>, respectively). The mechanism accelerating (i.e., during the abduction or adduction of the LPB filaments) and funneling (i.e., possible influence of maxillae or mandible positions) the water should be further analyzed.

In this study, the average PR evaluated for 4th instars of *Cs. morsitans* is ca. 48–58 times higher than the filtering rate evaluated by Aly (1988) for larvae of the same species and instar (0.136–0.164  $\mu\text{l}/\text{sec}$ ). Therefore, these results indicate that indirect estimation of filtration rates, from particle removal out of defined water volumes and time intervals, are most likely underestimates of the real water volume processed by the filtering structure(s). As a result, the actual feeding efficiency of this group is most likely lower than expected. Similar rationale, but opposite conclusions, were reached by Lacoursière and Craig (1993) for black fly larvae as they successfully established the amount of water processed by the filtering structures of the larvae (i.e., filtering efficiency was higher than expected because the volume processed was lower than originally calculated).

## CONCLUSIONS

Although great care must be applied when selecting video segments, water PRs of active suspension-feeding larvae can readily be estimated using the principle of continuity on the conical jet flow driving the large recirculation patterns surrounding the organisms. Examination of more species and associated instars are necessary before definitive conclusions can be made on the relative importance of morphologic and behavioral influences on PRs.

Overall flow analyses of the head vicinity did not support or provide an answer to the question of

whether, as suggested by Dahl et al. (1988), the jet is the result of a combined action of the LPBs and pharynx actions. However, the gathered observations strongly suggest that the constant water acceleration is solely produced and maintained by the sequential beating of the LPB filaments and that movements of the pharynx seem only to be associated with food-bowl formation and swallowing.

Further analyses of the functional aspect of suspension feeding are needed, because, as suggested by Koehl (1996), such studies are important tools for understanding relations between phenotype, behavior (e.g., differences in stroke frequency sensu Dahl et al. 1988, Widahl 1994), ecological performance, and success.

## ACKNOWLEDGMENTS

We are grateful to Douglas A. Craig for stimulating discussions and to Lena Vought for sharing interest and giving access to her laboratory and analytical facilities. The study was supported by The Swedish National Council (NFR) grant B-BU 3318–309 to C.D. The experiments were conducted at the Department of Zoology, Section of Entomology, Uppsala University, Uppsala, Sweden.

## REFERENCES CITED

- Aly, C. 1988. Filtration rates of mosquito larvae in suspensions of latex microsphere and yeast cells. *Entomol. Exp. Appl.* 46:55–61.
- Cheer, A. Y. L. and M. A. R. Koehl. 1987. Fluid flow through filtering appendages of insects. *IMA J. Math. Appl. Med. Biol.* 4:185–199.
- Dadd, R. H. 1968. A method for comparing feeding rates in mosquito larvae. *Mosq. News* 28:226–230.
- Dadd, R. H. 1971. Effects of size and concentration of particles on rates of ingestion of latex particulates by mosquito larvae. *Ann. Entomol. Soc. Am.* 64:687–692.
- Dadd, R. H. 1980. Feeding mechanisms and nutrition of mosquitoes. *Calif. Agric.* 1980:16.
- Dahl, C., L.-E. Widahl and C. Nilsson. 1988. Functional analysis of the suspension feeding system in mosquitoes

- (Diptera: Culicidae). *Ann. Entomol. Soc. Am.* 81:105–127.
- Dahl, C., G. Sahlén, J. Grawe, A. Johannisson and H. Amneus. 1993. Differential particle uptake in three species of mosquito larvae (Diptera: Culicidae). *J. Med. Entomol.* 30:537–543.
- Joergensen, C. 1983. Fluid mechanical aspects of suspension feeding. *Mar. Ecol. Prog. Ser.* 11:89–103.
- Koehl, M. A. R. 1994. Quantifying flow through dynamically scaled physical models suspension-feeding appendages. *Am. Zool.* 34:365. (abstract).
- Koehl, M. A. R. 1996. When does morphology matter? *Annu. Rev. Ecol. Syst.* 27:501–542.
- Lacoursière, J. and D. A. Craig. 1993. Fluid transmission and filtration efficiency of the labral fans of black fly larvae (Diptera: Simuliidae): hydrodynamic, morphological and behavioral aspects. *Can. J. Zool.* 71:148–162.
- Loudon, C. 1990. Empirical tests of filtration theory: particle capture by rectangular- mesh nets. *Limnol. Oceanogr.* 35:143–148.
- Merritt, R. W., R. H. Dadd and E. D. Walker. 1992a. Feeding behavior, natural food, and nutritional relationships of larval mosquitoes. *Annu. Rev. Entomol.* 37:349–376.
- Merritt, R. W., D. A. Craig, R. S. Wotton and E. D. Walker. 1996. Feeding behaviour of aquatic insects: case studies on black fly and mosquito larvae. *Invert. Biol.* 115:206–217.
- Merritt, R. W., D. A. Craig, E. D. Walker, H. A. Vanderploeg and R. S. Wotton. 1992b. Interfacial feeding behaviour and particle flow patterns of *Anopheles quadrimaculatus* larvae (Diptera Culicidae). *J. Insect Behav.* 5:741–761.
- Rashed, S. S and M. S. Mulla. 1989. Factors influencing ingestion of particulate materials by mosquito larvae (Diptera: Culicidae). *J. Med. Entomol.* 26:210–216.
- Shimeta, J. and P. A. Jumars. 1991. Physical mechanism and rates of particle capture by suspension-feeders. *Oceanogr. Mar. Biol. Annu. Rev.* 29:191–257.
- Shimeta, J. and M. A. R. Koehl. 1995. Mechanics and ecology of particle selection by tentaculate invertebrate suspension feeders; influences of ontogeny and ambient flow speed. *Am. Zool.* 35:549. (abstract).
- Shimeta, J. and M. A. R. Koehl. 1997. Mechanics of particle selection by tentaculate suspension feeders during encounter, retention and handling. *J. Exp. Mar. Biol. Ecol.* 209:47–73.
- Vanderploeg, H. A. 1990. Feeding mechanisms and particle selection in suspension-feeding zooplankton. p. 183–212. *In: R. S. Wotton (ed.). The biology of particles in aquatic systems.* CRC Press, Inc., Boca Raton, FL.
- Vogel, S. 1994. *Life in moving fluids. The physical biology of flow*, 2nd ed. Princeton University Press, Princeton, NJ.
- White, F. M. 1986. *Fluid mechanics*, 2nd ed. McGraw-Hill Book Co., New York.
- Widahl, L.-E. 1988. Some morphometric differences between container and pool breeding Culicidae. *J. Am. Mosq. Control Assoc.* 4:76–81.
- Widahl, L.-E. 1992. Flow patterns around suspension-feeding mosquito larvae (Diptera: Culicidae). *Ann. Entomol. Soc. Am.* 85:91–95.
- Widahl, L.-E. 1994. Production of flow patterns in mosquito larva (Diptera: Culicidae). *Ann. Entomol. Soc. Am.* 87:482–485.